Experimental and Theoretical Studies of Sodium Cation Interactions with the Acidic Amino Acids and Their Amide Derivatives

A. L. Heaton, R. M. Moision, and P. B. Armentrout*

Department of Chemistry, University of Utah, Salt Lake City, Utah 84112

Received: December 11, 2007; In Final Form: January 16, 2008

The binding of Na^+ to aspartic acid (Asp), glutamic acid (Glu), asparagine (Asn), and glutamine (Gln) is examined in detail by studying the collision-induced dissociation (CID) of the four sodiated amino acid complexes with Xe using a guided ion beam tandem mass spectrometer (GIBMS). Analysis of the energy-dependent CID cross sections provides 0 K sodium cation affinities for the complexes after accounting for unimolecular decay rates, internal energy of the reactant ions, and multiple ion−molecule collisions. Quantum chemical calculations for a number of geometric conformations of each Na^+(L) complex are determined at the B3LYP/6-311+G(d,p) level with single-point energies calculated at MP2(full), B3LYP, and B3P86 levels using a 6-311+G(2d,2p) basis set. This coordinated examination of both experimental work and quantum chemical calculations allows the energetic contributions of individual functionalities as well as steric influences of relative chain lengths to be thoroughly explored. Na^+ binding affinities for the amide complexes are systematically stronger than those for the acid complexes by 14 ± 1 kJ/mol, which is attributed to an inductive effect of the OH group in the carboxylic acid side chain. Additionally, the Na^+ binding affinity for the longer-chain amino acids (Glx) is enhanced by 4 ± 1 kJ/mol compared to the shorter-chain Asx because steric effects are reduced.

Introduction

Among the 20 naturally occurring amino acids, aspartic acid (Asp), asparagine (Asn), glutamic acid (Glu), and glutamine (Gln) play a critical role in the function of the P-type Na^+−K^+−ATPase enzyme, which is universal to all animal cells and necessary for the regulation of cell volume and cell potential. Structural models produced by homology to Ca^{2+}−ATPase,[1] backed by mutagenesis studies,[2] have resolved the cation binding sites of Na^+−K^+−ATPase at an atomic level. The metal coordination sites are governed by Asx and Glx amino acids as they have a high affinity for Na^+ and K^+, made possible by their functionality and flexible side-chain lengths. Thus, Asx and Glx binding interactions with alkali metal cations are critical to Na^+−K^+−ATPase function and specificity. Structurally, the acidic amino acids, Asp and Glu, have side chains composed of a carboxylic acid functionality preceded by one- and two-carbon linkages, respectively. Their amide derivatives, Asn and Gln, replace the terminal hydroxyl group with an amine, resulting in carboxamide functionality. Respective chain lengths of both Asx and Glx amino acids are conserved.

The mainstream approach to understanding alkali cation−protein interactions has been at the scale of oligopeptides. The difficulty with such large-scale studies lies in their limited ability to quantitatively investigate specific interactions with accuracy and precision. Consequently, the intricate and often complicated details of specific site binding interactions of alkali metal cations become difficult to elucidate on this scale. Our lab[3−7] and others[8−14] use a different methodology to understand the binding affinity of metal ions with more complicated systems. A "thermodynamic vocabulary" of specific alkali metal binding interactions with small-scale systems can be combined to help understand systems having much greater complexity.[15] The experimental method used in our work is gas-phase threshold collision-induced dissociation (TCID). Because complications resulting from solvent effects can be eliminated, measurement of gas-phase cation affinities is convenient and has the additional advantage of reflecting the intrinsic bond strengths between alkali metal cations and peptides. Further, this is an ideal venue for detailed comparison of experimental and theoretical results.

Some experimental data on sodium cation affinities for α-amino acids are available. High-pressure mass spectrometric experiments by Hoyau et al.[9] establish a series of accurate gas-phase sodium cation affinities of organic molecules with a wide variety of functional groups, though Asx and Glx are not included in this study. Studies by Bojesen et al.[13] determine the relative Na^+ binding to each of the 20 naturally occurring α-amino acids using Cooks's kinetic method[16,17] but do not provide absolute binding affinities for these substrates. Additionally, Kish et al.[14] determined relative sodium cation affinities of α-amino acids using Cooks's kinetic method based on the dissociation characteristics of collisionally activated Na^+ heterodimer complexes. This ladder of relative sodium cation affinities was converted to absolute BDEs by anchoring the values to the Na^+ affinity of Ala, which was determined by kinetic method experiments using three aliphatic amides as references, whose absolute Na^+ affinities were determined theoretically. Quantitative results of this study for Asx and Glx are discussed further below. No direct measurements of Na^+ binding to Asx and Glx have been accomplished previously.

In the work presented here, we expand our knowledge of sodium cation affinities by examining in detail the binding of the sodium cation to Asp, Glu, Asn, and Gln. Our approach in studying the four Asx and Glx amino acids concurrently is to better understand the energetic relevance of individual functionalities as well as the steric influences of chain length on

* To whom correspondence should be addressed.

10.1021/jp711649g CCC: $40.75
Published on Web 03/21/2008

sodium cation binding. We achieve a quantitative understanding of the impact that chelation, electron delocalization, inductive effects, and conformational strain have on the binding strength of all four ligands with sodium.

We provide here the first directly measured experimental values for Na^+ binding with Asp, Glu, Asn, and Gln. Absolute bond dissociation energies (BDEs) of the $Na^+(L)$ complexes are measured using TCID in a guided ion beam tandem mass spectrometer. Theoretical calculations at the B3LYP/6-311+G(d,p) level are carried out to provide structures, vibrational frequencies, and rotational constants needed for analysis of the TCID data. Experimental BDEs are compared to theoretical calculations performed for a number of possible $Na^+(L)$ geometries at the MP2(full)/6-311+G(2d,2p), B3LYP/6-311+G(2d,2p), and B3P86/6-311+G(2d,2p) levels using geometries and zero-point energy corrections calculated at the B3LYP/6-311+G(d,p) level of theory. This comparison helps identify the ground-state conformers being studied experimentally.

Experimental and Computational Section

General Experimental Procedures. Cross sections for CID of the metal−ligand complexes are measured using a guided ion beam tandem mass spectrometer that has been described in detail previously.[18,19] Studies of each $Na^+(L)$ complex are conducted using an electrospray ionization (ESI) source[20] under conditions similar to those described previously.[20] Briefly, the ESI is operated using a 50:50 by volume H_2O/MeOH solution with $\sim 10^{-4}$ M amino acid and NaCl (all chemicals purchased from Sigma-Aldrich), which is syringe-pumped at a rate of 0.04 mL/hr into a 35 gauge stainless steel needle biased at ~2000 V. Ionization occurs over the ~5 mm distance from the tip of the needle to the entrance of the capillary, biased at ~35 V. Ions are directed by a capillary heated to 80 °C into a radio frequency (rf) ion funnel,[21] wherein they are focused into a tight beam. Ions exit the ion funnel and enter a rf hexapole ion guide that traps them radially. Here, the ions undergo multiple collisions ($>10^4$) with the ambient gas and become thermalized.

The ESI source is assumed to produce ions having their internal energies well described by a Maxwell−Boltzmann distribution of rovibrational states at 300 K, as characterized in previous experiments.[20,22] Metal−ligand complexes are then extracted from the source and mass selected using a magnetic momentum analyzer. The mass-selected ions are decelerated to a well-defined kinetic energy and are focused into a rf octopole ion guide that traps the ions radially.[23,24] The ion guide minimizes losses of the reactant and any product ions resulting from scattering. The octopole passes through a static gas cell containing xenon, which is used as the collision gas for reasons described elsewhere.[25,26] After collision, the reactant and product ions drift to the end of the octopole where they are extracted and focused into a quadrupole mass filter for mass analysis. The ions are detected with a high-voltage dynode, scintillation ion detector, and the signal is processed using standard pulse counting techniques. Ion intensities, measured as a function of collision energy, are converted to absolute cross sections, as described previously.[18] The uncertainty in relative cross sections is about ±5%, and that for the absolute cross sections is about ±20%. The ion kinetic energy distribution is measured to be Gaussian and has a typical fwhm of 0.1−0.2 eV (lab) for the ESI source. Uncertainties in the absolute energy scale are about ±0.05 eV (lab). Ion kinetic energies in the laboratory frame are converted to energies in the center-of-mass (CM) frame using $E_{CM} = E_{lab}m/(m + M)$, where M and m are the masses of the ionic and neutral reactants, respectively. All energies herein are reported in the CM frame unless otherwise noted.

Thermochemical Analysis. Threshold regions of the CID reaction cross sections are modeled using eq 1

$$\sigma(E) = (n\sigma_0/E)\Sigma\, g_i \int_{E_0-E_i}^{E} (1 - e^{-k_{tot}(E^*)\tau})(E - \epsilon)^{n-1} d(\epsilon) \quad (1)$$

where σ_0 is an energy-independent scaling factor, n is an adjustable parameter that describes the efficiency of collisional energy transfer,[19] E is the relative kinetic energy of the reactants, E_0 is the threshold for dissociation of the ground electronic and rovibrational state of the reactant ion at 0 K, τ is the experimental time for dissociation ($\sim 5 \times 10^{-4}$ s in the extended dual octopole configuration as measured by time-of-flight studies),[19] ϵ is the energy transferred from translation during the collision, and E^* is the internal energy of the energized molecule (EM) after the collision, that is, $E^* = \epsilon + E_i$. The summation is over the rovibrational states of the reactant ions, i, where E_i is the excitation energy of each state and g_i is the fractional population of those states ($\sum g_i = 1$). The Beyer−Swinehart algorithm[27−29] is used to evaluate the number and density of the rovibrational states, and the relative populations g_i are calculated for a Maxwell−Boltzmann distribution at 300 K.

The term $k(E^*)$ is the unimolecular rate constant for dissociation of the energized molecule and is defined by Rice−Ramsperger−Kassel−Marcus (RRKM) theory as in eq 2[30,31]

$$k(E^*) = d N_{vr}^{\dagger}(E^* - E_0)/h\rho_{vr}(E^*) \quad (2)$$

where d is the reaction degeneracy, $N_{vr}^{\dagger}(E^* - E_0)$ is the sum of rovibrational states of the transition state (TS) at an energy $E^* - E_0$, and $\rho_{vr}(E^*)$ is the density of states of the energized molecule (EM) at the available energy, E^*. These rate constants allow kinetic shifts to be modeled, as discussed below.[32,33]

Several effects that obscure the interpretation of the data must be accounted for during data analysis in order to produce accurate thermodynamic information. The first effect involves energy broadening resulting from the thermal motion of the neutral collision gas and the kinetic energy distribution of the reactant ion. This is accounted for by explicitly convoluting the model over both kinetic energy distributions, as described elsewhere in detail.[18] The second effect considers that eq 1 only models cross sections that represent products formed as the result of a single collision event. To ensure rigorous single-collision conditions, data are collected at three pressures of Xe, generally about 0.16, 0.08, and 0.04 mTorr, and the resulting cross sections are evaluated for pressure effects and extrapolated to zero pressure when necessary.[34] The third effect arises from the lifetime for dissociation. As the size of reactant molecules increases, so do the number of vibrational modes of the reactant ion and thus the time for energy randomization into the reaction coordinate after collision. Thus, some energized molecules may not dissociate during the time scale of the experiment.[32] This leads to a delayed onset for the CID threshold, a kinetic shift, which becomes more noticeable as the size of the molecule increases. These kinetic shifts are estimated by the incorporation of RRKM theory as shown in eq 1 and as described in detail elsewhere.[32] To evaluate the rate constant in eq 1, sets of rovibrational frequencies for the EM and all TSs are required. Because the metal−ligand interactions in our $Na^+(L)$ complexes are mainly electrostatic, the most appropriate model for the TS for dissociation of the intact ligand is a loose association of the ion and neutral ligand fragments. The appropriateness of this assumption for multidentate ligands has been verified previously for crown ethers[7,35] and more recently for the tripeptide,

GlyGlyGly.[22] Therefore, these TSs are treated as product-like, such that the TS frequencies are those of the dissociation products. The molecular parameters needed for the RRKM calculation are taken from the quantum chemical calculations detailed in the next section. The transitional frequencies in the TSs are treated as rotors, a treatment that corresponds to a phase space limit (PSL), as described in detail elsewhere.[32,33] The 2D external rotations are treated adiabatically but with centrifugal effects included.[29] In the present work, the adiabatic 2D rotational energy is treated using a statistical distribution with an explicit summation over all of the possible values of the rotational quantum number.[32,33]

The model cross sections of eq 1 are convoluted with the kinetic energy distribution of the reactants and compared to the data. A nonlinear least-squares analysis is used to provide optimized values for σ_0, n, and E_0. The uncertainty associated with E_0 is estimated from the range of threshold values determined from different data sets with variations in the parameter n, variations in vibrational frequencies (±10% in most frequencies and a factor of 2 for the $Na^+(L)$ modes), changes in τ by factors of 2, and the uncertainty of the absolute energy scale, 0.05 eV (lab).

In deriving the final optimized BDEs at 0 K, two assumptions are made. First, we assume that there is no activation barrier in excess of the reaction endothermicity for the loss of ligands, which is generally true for ion−molecule reactions and for the heterolytic noncovalent bond dissociations considered here.[36] Second, the measured threshold E_0 values for dissociation are from ground-state reactant to ground-state ion and neutral ligand products. Given the relatively long experimental time frame ($\sim 5 \times 10^{-4}$ s), dissociating products should be able to rearrange to their low-energy conformations after collisional excitation.

Computational Details. The neutral ligands and metalated complexes of interest here may have numerous geometric conformations with relative energies close to the lowest-energy complex. To find the global minimum energy and all low-energy geometries, a large number of possible conformations were screened as follows.[37] A simulated annealing methodology using the AMBER suite of programs and the AMBER force field[38] was used to generate starting structures for higher-level optimizations. All unique structures generated via simulated annealing were further optimized using NWChem[39] at the HF/321G level. For these alkali cation/amino acid complexes, we have found that energies determined with this low-level ab initio calculation show a higher correlation with energies calculated at higher levels of theory than that with the relative energies from the AMBER force field. All unique structures from the HF/3-21G calculations within about 30 kJ/mol of the lowest-energy structure ($\sim$10 structures for each $Na^+(L)$ complex) were further optimized using Gaussian 03[40] at the B3LYP/6-31G(d) level with "loose" optimization (maximum step size of 0.01 au and a rms force of 0.0017 au) to facilitate more rapid convergence. All unique structures were then optimized at the B3LYP/6-311+G(d,p) level. Rotational constants were obtained from the optimized structures, and vibrational frequencies were also calculated at this level. When used in internal energy determinations or for RRKM calculations, the vibrational frequencies were scaled by 0.99.[41] Single-point energies were calculated at the MP2(full), B3LYP, and B3P86 levels using the 6-311+G(2d,2p) basis set and the B3LYP/6-311+G(d,p) geometries. Zero-point vibrational energy (ZPE) corrections were determined using the scaled vibrational frequencies. Basis set superposition errors (BSSE) were estimated using the full counterpoise (cp) method.[42,43] For the MP2 single-point energies, the BSSE corrections range from 13 to 14 kJ/mol, whereas for the B3LYP and B3P86 single-point energies, they range between 3 and 4 kJ/mol for all structures examined here. This is consistent with previous observations by this lab[3,37] and others[44] that BSSE corrections for DFT calculations on alkali metal cation systems are generally small. Feller and co-workers[45,46] and Ohannesian and co-workers[9,10] have previously commented that the full counterpoise approximation to BSSE can provide worse agreement with experiment than with theoretical values without BSSE corrections. Because of this possibility for BSSE to overcorrect the MP2 calculations, the "best" MP2 values may fall between the MP2 values with and without BSSE corrections. Therefore, both values are reported here. All of the absolute binding energies obtained using DFT calculations reported here include BSSE corrections.

Results

Cross Sections for Collision-Induced Dissociation. Kinetic-energy-dependent experimental cross sections were obtained for the interaction of Xe with $Na^+(L)$, where L = Asp, Glu, Asn, and Gln. Figure 1 shows representative data sets for all four $Na^+(L)$ systems. Data shown are a mean of results taken at xenon pressures of $\sim$0.04, 0.08, and 0.16 mTorr, as no pressure dependence for these systems was observed. At high energies, the most favorable process observed for all complexes is the loss of the intact ligand in the collision-induced dissociation (CID) reaction 3

$$Na^+(L) + Xe \rightarrow Na^+ + L + Xe \quad (3)$$

The $Na^+(Asp)$ system shows no additional competing pathways, whereas the $Na^+(Asn)$ system also exhibits formation of a product ion corresponding to loss of NH_3 from the intact complex, designated as $Na^+(Asn-NH_3)$, in reaction 4

$$Na^+(Asn) + Xe \rightarrow Na^+(Asn-NH_3) + NH_3 + Xe \quad (4)$$

The $Na^+(Glu)$ system also shows one decomposition channel in addition to reaction 3, forming a product corresponding to H_2O loss, reaction 5. Likewise, $Na^+(Gln)$ exhibits a product ion having the same mass, which corresponds to NH_3 loss, reaction 6, as well as a H_2O loss channel, reaction 7

$$Na^+(Glu) + Xe \rightarrow Na^+(Glu-H_2O) + H_2O + Xe \quad (5)$$

$$Na^+(Gln) + Xe \rightarrow Na^+(Gln-NH_3) + NH_3 + Xe \quad (6)$$

$$\rightarrow Na^+(Gln-H_2O) + H_2O + Xe \quad (7)$$

Interestingly, the loss of ammonia from asparaginyl and glutaminyl residues has been linked to the process of biological aging.[47,48] Furthermore, HX loss from Glx, where X = OH for Glu and NH_2 for Gln, can produce oxo-proline (O-Pro), which is significant biologically and has been identified as the N-terminal amino acid of a large number of naturally occurring proteins.[49] Thus, a more detailed analysis of the observed minor channels in the future should be of interest; however, these analyses require knowledge of the reaction paths and transition states for these decompositions (which are likely to be tight TSs on the basis of their kinetic energy behavior). Therefore, they are beyond the scope of the present study, although additional experiments relevant to these decomposition reactions are presented in the following paper.[50]

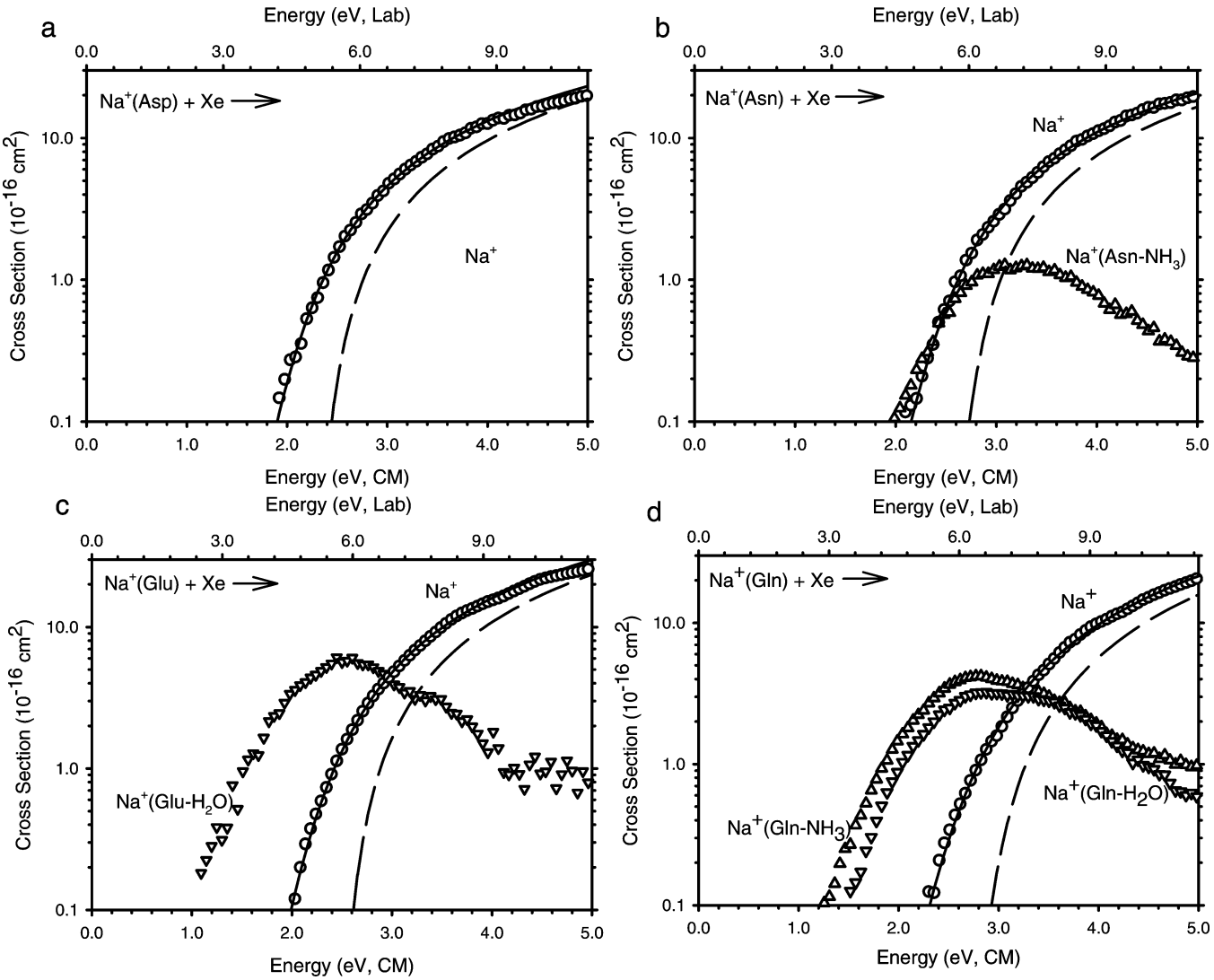

Figure 1. Cross sections for collision-induced dissociation of $Na^+(L)$, where L = aspartic acid, asparagine, glutamic acid, and glutamine (parts a−d, respectively), with Xe as a function of kinetic energy in the center-of-mass frame (lower *x*-axis) and the laboratory frame (upper *x*-axis). Solid lines show the best fit to the data using the model of eq 1 convoluted over the neutral and ion kinetic and internal energy distributions. Dashed lines show the model cross sections in the absence of experimental kinetic energy broadening for reactants with an internal energy of 0 K.

In the Na^+(Asx) systems, all minor pathways have maximum cross sections over 1 order of magnitude smaller than those for loss of Na^+. For the Na^+(Glx) systems, the minor pathways have larger cross sections than those in the Na^+(Asx) systems but are still a factor of 5 smaller than those for reaction 3 at their maxima. It is possible that competition between the two channels may cause a shift in the measured thresholds for reaction 3; however, given the intensity of the minor channels and the probability that each minor pathway goes through a tight transition state, the loose TS product associated with reaction 3 quickly dominates such that any competitive shift is expected to be within our conservative experimental uncertainty. For this and other reasons outlined elsewhere,[5] we have ignored these reactions in our analyses of the thresholds for reaction 3. The reasonableness of this assumption has been verified in the similar case of Na^+(GlyGlyGly)[22] and in a preliminary competitive analysis of the present systems.

The model of eq 1 was used to analyze the thresholds for reaction 3 for the four Na^+(L) systems. Figure 1 shows that all experimental cross sections are reproduced by eq 1 over a large range of energies (~3 eV) and magnitudes (greater than 2 orders of magnitude). The optimized fitting parameters of eq 1 are provided in Table 1. Modest kinetic shifts are observed and

TABLE 1: Fitting Parameters of Equation 1, Threshold Dissociation Energies at 0 K, and Entropies of Activation at 1000 K for CID of Na^+(L)[a]

reactant	σ_0	n	E_0 (eV) no RRKM	E_0 (PSL) (eV)	$\Delta S^{\ddagger}_{1000}$ (J/K/mol)
Na^+(Asp)	15.2 (1.6)	1.9 (0.1)	2.33 (0.09)	2.02 (0.06)	52 (2)
Na^+(Glu)	20.7 (3.8)	1.9 (0.1)	2.48 (0.06)	2.06 (0.05)	70 (2)
Na^+(Asn)	18.8 (1.8)	1.8 (0.1)	2.62 (0.10)	2.17 (0.06)	42 (2)
Na^+(Gln)	16.2 (2.8)	2.0 (0.2)	2.76 (0.10)	2.21 (0.06)	58 (2)

[a] Uncertainties in parentheses.

range from about 0.3 eV for Na^+(Asp), the most weakly bound system, to almost 0.6 eV for the strongly bound Na^+(Gln) complex. This trend is consistent with previous observations that kinetic shifts track with increasing threshold energy and ligand complexity. From our analyses, we also derive values of $\Delta S^{\ddagger}_{1000}$, the entropy of activation at 1000 K, which give some idea of the looseness of the transition states. These values, listed in Table 1, are in the range determined by Lifshitz[51] for simple bond cleavage dissociations. This is reasonable considering that the TS is assumed to lie at the centrifugal barrier for the association of $Na^+ + L$. The rotational contributions to $\Delta S^{\ddagger}_{1000}$ are fairly constant for the complexes studied here. The moderate

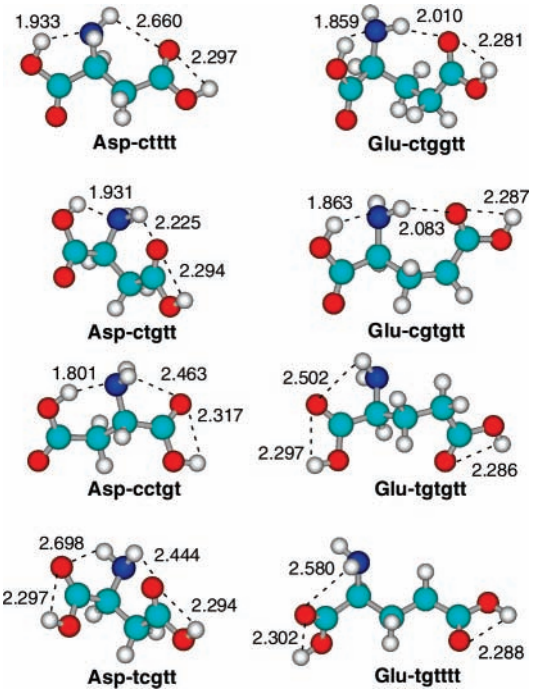

Figure 2. Ground- and excited-state conformations of neutral Asp and Glu calculated at the B3LYP/6-311+G(d,p) level of theory. Hydrogen bond lengths are shown in Å.

TABLE 2: Relative Energies (kJ/mol) for Conformers of Neutral Asx and Glx[a]

species	B3LYP	B3P86	MP2 (full)	species	B3LYP	B3P86	MP2 (full)
Asp-ctttt	0.0	0.0	1.4	Glu-ctggtt	0.7	0.0	1.3
ctgtt	2.0	1.7	0.0	cgtgtt	0.9	0.6	3.5
cctgt	3.6	3.4	4.3	tgtgtt	0.3	4.0	0.0
tcgtt	4.5	7.5	0.4	tgtttt	0.0	5.0	2.7
Asn-ctgg	0.0	0.0	0.0	Gln-ctggt	0.0	0.0	2.5
cttt	2.2	3.2	7.6	cgtgt	1.8	1.8	6.5
cggt	4.0	5.1	8.7	cg_+ggg	2.1	2.5	0.0
cgtg	3.1	4.9	9.5	cg_-ggg	3.8	4.8	1.9

[a] Structures and zero-point energies determined at the B3LYP/6-311+G(d,p) level with B3LYP, B3P86, and MP2(full) single-point energies determined using a 6-311+G(2d,2p) basis set.

variations observed in the $\Delta S^{\ddagger}_{1000}$ values are the result of vibrational contributions from the different TS geometries.

Theoretical Results for Sodiated Amino Acid Complexes. Structures of the four neutral amino acids experimentally studied here and for the complexes of these species with Na^+ were calculated as described above. A number of low-energy conformations are possible for the neutral structures. Structures for the four lowest-energy conformations of neutral Asp and Glu are provided in Figure 2. Structures for Asn and Gln are generally similar to those for Asp and Glu, respectively, and are provided in Figure S1 in the Supporting Information. Structures are named by the series of dihedral angles starting from the carboxylic acid hydrogen of the backbone and going to the terminal R-group hydrogen for the acids and terminal R-group nitrogen for the amides. The dihedral angles are distinguished as cis (c, for angles between 0 and 45°), gauche (g, 45−135°), or trans (t, 135−180°). Relative energies of the low-energy conformations of all four amino acids are provided in Table 2 and lie within 10 kJ/mol at all levels of theory. The low-energy conformations of all of these neutral ligands are stabilized by 3−4 intramolecular hydrogen bonds, as shown in Figures 2 and S1, and these associations can occur in a number of ways to attain comparable stabilization. Indeed, the energy difference between conformers is sufficiently small that different levels of theory can disagree on the ground-state (GS) conformation for the ligands. The most extreme case is for glutamic acid, where the B3LYP, B3P86, and MP2(full) calculations each designate a different structure as the GS, Table 2.

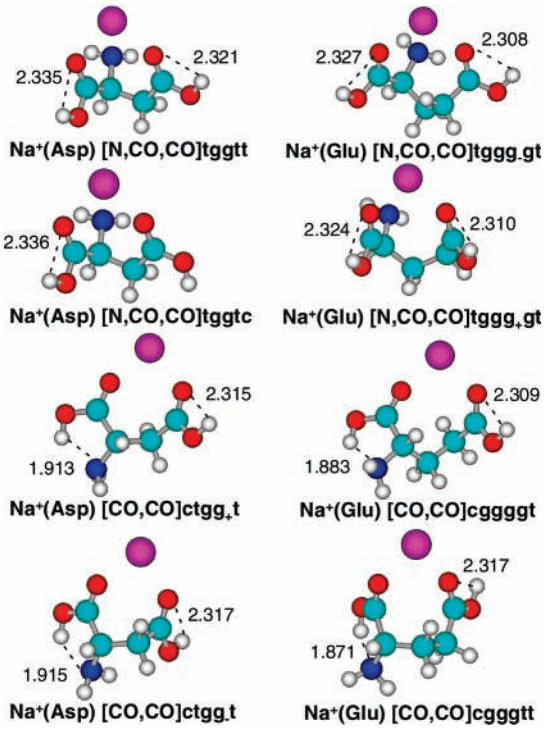

Figure 3. Ground- and excited-state conformations of sodiated Asp and Glu calculated at the B3LYP/6-311+G(d,p) level of theory. Hydrogen bond lengths are shown in Å.

Complexation of Na^+ to these ligands introduces some distortions of the neutral ligand structures and does so in such a way to clearly delineate a GS conformation among the possible conformers, Figures 3 (Asp and Glu) and S2 (Asn and Gln). Structures are named by their binding sites to the sodium cation (in brackets) and by the series of dihedral angles as per the neutral ligand. Key structural parameters and the relative energies of the four lowest-energy conformations are provided in Table 3.

For Asp, the GS structure, [N,CO,CO]tggtt, has a tridentate conformation in which the metal ion binds to the backbone carbonyl and amine as well as to the side-chain carbonyl. [N,CO,CO]tggtc lies about 20 kJ/mol higher in energy and has an analogous structure minus the hydrogen bond in the side-chain COOH group. The next two Na^+(Asp) structures lie 21−30 kJ/mol above the GS, each having bidentate binding to both carbonyl oxygens, [CO,CO]. They are similar in energy, differing structurally only in the sign of the ∠C−C−C−O gauche dihedral angle. For the Na^+(Asn) complexes, the GS is again tridentate, [N,CO,CO]tggt, whereas the three structures next highest in energy are all [CO,CO] bidentate. These structures are comparable in energy, lying 20−33 kJ/mol above the GS, Table 3.

For the longer-chain amino acids (Glx), there are two [N,CO,CO] tridentate Na^+ binding structures that differ only in the conformation of the molecule chain. For both Na^+(Glu) and Na^+(Gln), these two conformers have ∠NC−C−C−C dihedral angles that differ only in sign. These two tridentate conformations for each Na^+(Glx) complex differ in energy by only 1−5 kJ/mol, Table 3. The structures next highest in energy,

TABLE 3: Bond Distances (Å), Bond Angles (°), and Relative Energies (kJ/mol) for Low-Energy Structures of Sodiated Asx and Glx[a]

species	$r(Na^+-O)^b$	$r(Na^+-N)$	$r(Na^+-O)^c$	$\angle(NNaO^b)$	$\angle(NNaO^c)$	$\angle(O^bNaO^c)$	B3LYP	B3P86	MP2(full)
Na^+(Asp) [N,CO,CO]tggtt	2.304	2.480	2.274	70.1	79.4	88.3	0.0	0.0	0.0
[N,CO,CO]tggtc	2.317	2.501	2.255	69.2	78.3	87.3	20.5	20.1	19.5
[CO,CO]ctgg$_+$t	2.182		2.315			84.7	22.1	21.2	29.7
[CO,CO]ctgg$_-$t	2.201		2.281			84.7	24.2	21.3	26.9
Na^+(Asn) [N,CO,CO]tggt	2.318	2.479	2.230	69.8	79.6	88.3	0.0	0.0	0.0
[CO,CO]ctg$_+$g	2.215		2.229			84.3	22.2	21.6	32.5
[CO,CO]ctg$_-$g	2.184		2.196			86.6	23.7	20.8	27.7
[CO,CO]cggt	2.186		2.196			86.0	24.0	22.2	31.6
Na^+(Glu) [N,CO,CO]tggg$_-$gt	2.300	2.496	2.244	70.1	84.0	105.9	0.0	0.0	0.0
[N,CO,CO]tggg$_+$gt	2.293	2.511	2.250	69.3	92.9	87.5	4.7	4.3	3.2
[CO,CO]cggggt	2.177		2.249			90.7	10.9	7.5	14.1
[CO,CO]cgggtt	2.185		2.237			86.1	14.7	10.5	16.7
Na^+(Gln) [N,CO,CO]tggg$_-$g	2.310	2.468	2.202	70.7	83.4	103.9	0.0	0.0	0.0
[N,CO,CO]tggg$_+$g	2.298	2.507	3.380	69.1	91.4	87.7	3.7	3.0	1.1
[CO,CO]cgtgt	2.198		2.194			100.4	9.0	5.2	15.4
[CO,CO]cgggg	2.188		2.199			93.0	13.6	10.3	16.8

[a] Structures calculated at the B3LYP/6-311+G(d,p) level of theory. Single-point energies determined at B3LYP, B3P86, and MP2(full)/6-311+G(2d,2p)//B3LYP/6-311+G(d,p). [b] Carbonyl oxygen of the amino acid backbone. [c] Carbonyl oxygen of the amino acid side chain.

both bidentate [CO,CO] associations, lie 5−17 kJ/mol higher than the GS.

The distortions that occur upon Na^+ complexation to stabilize these flexible ligands are rather extreme. Many of the intramolecular hydrogen bonds present in the ground-state conformations of the neutral ligands must be broken to allow the atoms involved in these associations to stabilize the positively charged sodium cation instead. For low-energy conformations of all sodium cation complexes, it is clear that the carbonyl oxygens of the carboxylic acid and carboxamide functionalities quickly rearrange to help solvate the alkali metal ion. For the GS conformation of each Na^+(L) complex, the amine nitrogen of the amino acid backbone also participates to form a tridentate complex. Steric strain results from the formation of these tridentate associations, but the energetic trade-off appears favorable, as the calculations show that the tridentate conformers of each complex are lower in energy than the lowest-energy bidentate complexes where steric strain is reduced (as indicated by generally shorter Na^+-O bond distances for the bidentate complexes, Table 3). The steric strain is also reduced for the longer-chain Glx amino acids relative to Asx, as the longer chain allows unfavorable steric interactions with neighboring atoms to be minimized. This can be demonstrated by comparing the angles of Na^+ binding in the ground-state structures for Na^+(Asx) and Na^+(Glx). The optimal arrangement for tridentate binding to Na^+ is a trigonal planar arrangement with angles of 120°; yet, the nonplanar arrangement of our amino acid complexes produces notably smaller angles, Table 3. For each GS complex, the binding angles between the amino nitrogen of the backbone and both the backbone and side-chain carbonyl oxygens are comparable, ∼70 and ∼80°, respectively. Yet, binding angles between the carbonyl oxygens are systematically smaller for Asx (∼88°) than those for Glx (∼105°) because of steric limitations of the shorter Asx chain length. As shown below, the more optimal binding angles in the GSs of Na^+(Glx) lead to a 4 ± 1 kJ/mol increase in binding affinity of the longer-chain Glx amino acids to the sodium cation compared to the shorter-chain Asx amino acids.

Discussion

Conversion from 0 to 298 K and Excited Conformers. Conversion from 0 K bond energies to 298 K bond enthalpies and free energies is accomplished using the rigid rotor/harmonic oscillator approximation with rotational constants and vibrational frequencies calculated at the B3LYP/6-311+G(d,p) level. These ΔH_{298} and ΔG_{298} values along with the conversion factors and 0 K enthalpies measured here are reported in Table 4. The uncertainties listed are determined by scaling most of the vibrational frequencies by ±10% along with twofold variations in the metal−ligand frequencies. We also calculated the ΔG_{298} values for the second lowest-energy structure of all Na^+(L) systems. In general, the relative ΔG_{298} excitation energies are comparable to the analogous differences in the ΔH_0 values, Table 3.

TABLE 4: Enthalpies and Free Energies of Sodium Binding at 0 and 298 K (kJ/mol)[a]

complex	$\Delta H_0{}^b$	$\Delta H_{298} - \Delta H_0{}^c$	ΔH_{298}	$T\Delta S_{298}{}^c$	ΔG_{298}
Na^+(Asp)	195 (6)	2.3 (0.3)	197 (6)	36.4 (4.3)	161 (7)
Na^+(Glu)	199 (5)	1.5 (0.2)	201 (5)	33.8 (4.8)	167 (7)
Na^+(Asn)	209 (6)	1.9 (0.2)	211 (6)	36.1 (4.3)	175 (7)
Na^+(Gln)	213 (6)	2.3 (0.3)	215 (6)	38.0 (4.5)	177 (8)

[a] Uncertainties in parentheses. [b] Experimental values from Table 1. [c] Calculated using standard formulas and molecular constants calculated at the B3LYP/6-311+G(d,p) level.

The theoretical BDEs discussed below are all calculated for the most stable Na^+(L) conformation. For some of the systems, it is possible that the complexes formed experimentally in the source region at thermal energies may consist of multiple low-energy conformers. Although no obvious evidence for multiple conformers is found experimentally, the sensitivity of TCID experiments to low-energy species is not particularly acute. Using the ΔG_{298} values to calculate an equilibrium population of conformers shows that the calculated GS structures for most Na^+(L) systems should be dominant in the room-temperature ion sources. Excited conformers for the Na^+(Asx) systems are calculated to comprise <0.1% of the total population, whereas excited conformers for the Na^+(Glu) and Na^+(Gln) systems are calculated to comprise 21−43% of the total population (depending on the level of theory). To investigate the effect of having a different conformer populating the Na^+(Glx) reactant ions, we reanalyzed the data using the molecular parameters of the second lowest-energy structure for the Na^+(Glx) systems. The threshold energies change by less than 1 kJ/mol in all cases, an effect that is included in the experimental uncertainties listed in the tables. Thus, even if there are multiple conformers present

TABLE 5: Experimental and Theoretical Sodium Affinities at 0 K (kJ/mol)

complex	experiment[a]	B3LYP[b,c]	B3P86[b,c]	MP2(full)[b]	MP2(full,cp)[b,c]	literature[d]
Na^+(Asp)	195 (6)	202	194	204	191	201 (8)
Na^+(Glu)	199 (5)	208	201	208	194	202 (8)
Na^+(Asn)	209 (6)	220	210	216	203	204 (8)
Na^+(Gln)	213 (6)	227	216	227	213	210 (8)
MAD[e]		10 (3)	2 (1)	10 (3)	4 (3)	

[a] Present experimental values from Table 1. Uncertainties in parentheses. [b] Calculations performed at the stated level of theory using a 6-311+G(2d,2p) basis set with geometries calculated at B3LYP/6-311+G(d,p) level. [c] Counterpoise corrected. [d] Kinetic method results from Kish et al.[14] [e] Mean absolute deviation from present experimental values.

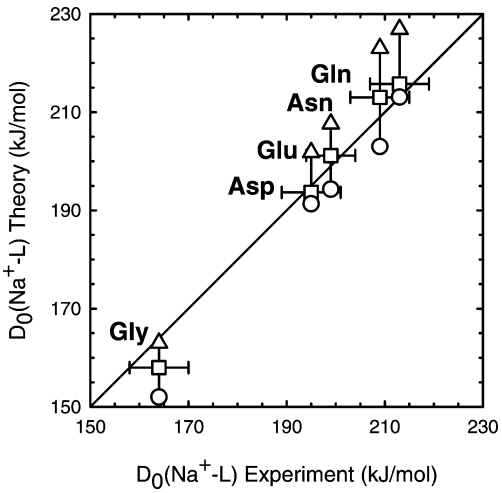

Figure 4. Experimental and theoretical bond energies (kJ/mol) of sodium cations bound to the four amino acids and Gly.[37] Theoretical values include those calculated at the B3LYP (triangles), B3P86 (squares), and MP2(full,cp) (circles) levels. Asx and Glx values are from Table 5.

in the reactant ion beams, this does not affect the thermochemistry derived within the stated experimental uncertainties.

Comparison of Experimental, Theoretical, and Literature Values. The sodium cation affinities for the four molecules examined in this study as measured using TCID with the guided ion beam mass spectrometer and calculated here are summarized in Table 5 and Figure 4. The sodium cation affinity of glycine, $D_0(Na^+-Gly) = 164 \pm 6$ kJ/mol,[37] is additionally provided in Figure 4 for comparison. The calculated binding energies refer to the ground-state conformations of each system. The agreement between theory and experiment for the Asx and Glx amino acids is extremely good. Theoretical calculations span the range of our experimentally determined values in all cases. Of this range, the values determined theoretically at the MP2(full) level including counterpoise corrections fall consistently below experimental values, with a mean absolute deviation (MAD) of 4 kJ/mol. By comparison, MP2(full) calculations excluding counterpoise give worse agreement and are systematically high, with a MAD of 10 kJ/mol. Overall, the utility of BSSE corrections appears advantageous in these systems. Values calculated at the B3P86 level yield values that are in excellent agreement with experiment, with a MAD of only 2 kJ/mol. Last, values calculated at the B3LYP level are systematically higher than experimentally determined values, with a MAD of 10 kJ/mol. This is consistent with previous work in our lab for a large number of Na^+(L) complexes, in which B3LYP methods usually result in sodium cation affinities higher than experimental values by about 8 kJ/mol.[3] All of these variations are comparable to the average experimental uncertainty of ~6 kJ/mol.

Sodium cation binding affinities for the four amino acids were determined by Kish et al.[14] using Cook's kinetic method relative to that of Ala (167 ± 8 kJ/mol), which was put on an absolute scale by kinetic method measurements of the sodium cation binding affinity of Ala relative to three aliphatic amides with absolute binding energies determined theoretically. Their values at 298 K are Na^+(Asp) = 203, Na^+(Glu) = 204, Na^+(Asn) = 206, and Na^+(Gln) = 212 kJ/mol, all with relative uncertainties of ±4 kJ/mol and absolute uncertainties of ±8 kJ/mol. When adjusted to 0 K using the data in Table 4 for comparison with our results, the BDEs become 201, 202, 204, and 210 ± 8, respectively. These BDEs are in rough agreement with our experimentally determined values, falling within combined experimental errors; however, the trends in these values do not match those of our TCID values or theoretical predictions. Specifically, our experiments find that the range of sodium cation affinities spanned by the four amino acids is 18 kJ/mol, whereas the range determined by the kinetic method is much smaller, only 9 kJ/mol, a difference outside of the stated uncertainty in the relative values of ±4 kJ/mol. Theory predicts ranges of 22−25 kJ/mol, Table 5, in reasonable agreement with our experimental results. Further, our studies designate that the longer chain length of Glx compared to that of Asx increases the Na^+ binding affinity by a systematic 4 ± 1 kJ/mol, whereas theory predicts an average change of 7 ± 3 kJ/mol. Also, the carboxamide versus carboxylic acid side-chain functionality increases the Na^+ binding affinity by a systematic 14 ± 1 kJ/mol in our experiments, whereas theory predicts an average difference of 16 ± 3 kJ/mol. The BDEs of Kish et al.[14] show no systematic trends for Na^+ binding as a function of chain length or functionality.

Qualitative Trends. The amino acids examined in this study can be broken down in two different ways, by functionality and chain length. Asp and Glu have a terminal carboxylic acid side-chain group, whereas Asn and Gln have a terminal carboxamide group. Asp and Asn have a shorter-chain side group, whereas Glu and Gln have a longer-chain side group. Previous work has shown that there are a number of factors that can influence the strength of Na^+ binding.[4−7,9,15] These include the nature of the donor atom, the localization of the electron density on the donor (orbital overlap with the metal ion), electrostatic interactions (polarizability, charge−dipole, and charge−quadrupole), and the possibility of multiple donor (chelation) interactions. For a hard ion such as Na^+, one expects the binding to be primarily electrostatic. We have noted before that species such as NH_3, CH_3NH_2, and $C_3H_7NH_2$ bind to Na^+ more strongly than the analogous H_2O, CH_3OH, and C_3H_7OH ligands.[4,37,52] Binding to a carbonyl group is favored even more, but when this functionality is part of a carboxylic acid group, the binding energy is reduced.[37]

The ground-state conformation of each amino acid complex studied here binds the sodium cation in a tridentate association. The additional stabilization achieved by complexation to the side chain compared to the bidentate conformation of GS Na^+(Gly), [N,CO], $D_0(Na^+-Gly) = 164 \pm 6$ kJ/mol,[37] is 31−49 ± 8 kJ/mol, Figure 4. This is considerably less than the binding affinity of a free carboxylic acid, $D_0(Na^+-CH_3CH_2-$

COOH) = 118 ± 6 kJ/mol,[37] which is the result of the multiple ligation combined with the less optimal geometry necessitated by the amino acid connectivity. Comparison of the sodium cation complexes of the acidic amino acids with the sodium cation complexes of their amide derivatives shows that the former complexes are more weakly bound than the latter complexes by 14 ± 1 kJ/mol, Figure 4 and Table 5. The weaker binding of the acidic amino acid complexes provides evidence that electron-withdrawing effects of the OH group in the carboxylic acid reduce the binding to Na^+. This effect of the reduced binding affinity of the carbonyl oxygen of a carboxylic acid functionality has been observed previously in TCID studies by Moision,[37] wherein the sodium cation was found to bind the carbonyl oxygen of CH_3CH_2COOH more weakly than the carbonyl oxygen of $CH_3CH_2COCH_3$ by 13 kJ/mol, very similar to the 14 ± 1 kJ/mol effect observed here. Further, the longer-chain amino acids can effectively solvate Na^+ with less steric strain than the shorter-chain amino acids, as discussed above. This is exhibited by the 4 ± 1 kJ/mol increase in the binding affinity of the longer-chain amino acids to the sodium cation compared to the shorter-chain amino acids.

Conclusion

The kinetic energy dependence of the collision-induced dissociation of $Na^+(L)$, L = aspartic acid, glutamic acid, asparagine, and glutamine, with Xe are examined in a guided ion beam mass spectrometer. Complexes of the intact amino acids with the sodium cation are readily formed in an ESI ion source. Thresholds at 0 K for the Na^+ affinity of the Asx and Glx amino acids are determined after consideration of the effects of reactant internal energy, multiple collisions with Xe, and lifetime effects using a phase space limit transition-state model.[32] The experimental binding energies are in excellent agreement with quantum chemical calculations using the B3P86/6-311+G(2d,2p)//B3LYP/6-311+G(d,p) level of theory. Values reported here for Asp, Glu, Asn, and Gln constitute the first direct experimental measurements of these sodium cation binding affinities.

The experimental results supported by theoretical calculations permit a systematic evaluation of the binding motifs of each $Na^+(L)$ complex, thereby allowing a dissection of binding trends relevant to group specificity and conformational mobility. For each $Na^+(L)$ complex, it is clear that the best binding motif is a tridentate association with both carbonyl oxygens along with the amino nitrogen of the backbone; however, when the side-chain carbonyl oxygens are part of a carboxylic acid functionality, the binding energy is reduced by 14 ± 1 kJ/mol. Enhancement of the binding affinity by 4 ± 1 kJ/mol is provided by lessened steric strain associated with the longer side-chain lengths of Glu and Gln compared to the shorter side-chain lengths of Asp and Asn. These systematic trends, consistent with theoretical calculations, are not evident in the available literature values,[14] even though the latter are within combined experimental errors of the present BDEs.

Note Added in Proof. Williams and co-workers have previously examined the structures of $M^+(Gln)$($M^+ = Li^+$ and Na^+) theoretically (Lemoff, A. S.; bush, M. F.; Wu, C.-C.; Williams, E. R. *J. Am. Chem. Soc.* **2005**, *127*, 10276). Using B3LYP/6-31G(d), B3LYP/6-31+G(d), and B3LYP/6-31++G(d,p) levels of theory, they located the same ground-state structure for $Na^+(Gln)$ as that in the present work, along with seven other higher-energy structures, most of which are considerably higher in energy than the four structures considered here. They did not locate the alternate [N,CO,CO] conformer discussed in the present work, nor did they mention the two [CO,CO] structures found here. However, they found a zwitterionic structure [CO_2^-] and its charge-solvated analogue [COOH] to be only 11.7 and 11.7 kJ/mol, respectively, above the ground state at a B3LYP/6-31G(d) level of theory and the zwitterion to lie 8.1 kJ/mol higher at a B3LYP/6-31++G(d,p) level.

At a B3LYP/6-311+G(d,p) level of theory, we located two low-lying zwitterionic sturctures for $Na^+(Gln)$, [CO_2^-]ggt and [CO_2^-]tgt, as well as the [COOH]ggt structure. At the B3LYP, B3P86, and MP2(full) levels of theory using a 6-311+G(2d,2p) basis set, we found that [CO_2^-]ggt lies 7.5, −0.2, and 9.0 kJ/mol above the [N,CO,CO] ground state, [CO_2^-]tgt lies 7.6, 0.6, and 11.9 kJ/mol above the ground state, and [COOH]ggt lies 47.4, 37.3, and 50.0 kJ/mol above the ground state. Likewise, we located several zwitterionic structures for $Na^+(Glu)$, two of which are low in energy, [CO_2^-]ggtt and [CO_2^-]tgtt, and have comparable excitation energies as their $Na^+(Gln)$ analogues. For completeness, we also located the zwitterionic structures for $Na^+(Asp)$ and $Na^+(Asn)$ and found that they lie 19−25 and 16−24 kJ/mol above their respective ground conformers. Details for all these structures and their energies can be found in the Supporting Information.

In no case does the possible presence of such zwitterionic conformations change the thermochemistry measured here. The B3P86 level of theory suggests that these species could be present experimentally for $Na^+(Glu)$ and $Na^+(Gln)$, whereas B3LYP and MP2(full) theory suggest they are too high in energy to be populated appreciably. Furthermore, the observation of the systematic variations in the sodium cation affinities among Asp, Asn, Glu, and Gln, as discussed in the text, suggests that the likely ground-state structures of $Na^+(Glu)$ and $Na^+(Gln)$ are tridentate [N,CO,CO], rather than zwitterionic [CO_2^-]. This conclusion is also consistent with the study of Williams and co-workers that $(H_2O)_xNa^+(Gln)$ complexes (x = 1 and 2) do not have zwitterionic structures (Lemoff, A. S.; Bush, M. F.; Wu, C.-C.; Williams, E. R. *J. Am. Chem. Soc.* **2005**, *127*, 10276; Lemoff, A. S.; Wu, C.-C.; Bush, M. F.; Williams, E. R. *J. Phys. Chem. A* **2006**, *110*, 3662).

Acknowledgment. This work is supported by the National Science Foundation. A grant of computer time from the Center for High Performance Computing at the University of Utah is gratefully acknowledged.

Supporting Information Available: Table of geometric parameters and relative energies of zwitterionic conformations of $Na^+(Asp)$, $Na^+(Asn)$, $Na^+(Glu)$, and $Na^+(Gln)$. Figures showing low-energy conformations of Asn, Gln, $Na^+(Asn)$, $Na^+(Gln)$, and zwitterionic conformations of $Na^+(Asp)$, $Na^+(Asn)$, $Na^+(Glu)$, and $Na^+(Gln)$. This material is available free of charge via the Internet at http://pubs.acs.org.

References and Notes

(1) Ogawa, H.; Toyoshima, C. *Proc. Natl. Acad. Sci. U.S.A.* **2002**, *99*, 15977.

(2) Jorgensen, P. L.; Hakansson, K. O.; Karlish, S. J. D. *Annu. Rev. Physiol.* **2003**, *65*, 817.

(3) Armentrout, P. B.; Rodgers, M. T. *J. Phys. Chem. A* **2000**, *104*, 2238.

(4) Rodgers, M. T.; Armentrout, P. B. *Mass Spectrom. Rev.* **2000**, *19*, 215.

(5) Rodgers, M. T.; Armentrout, P. B. *J. Phys. Chem. A* **1999**, *103*, 4955.

(6) Amicangelo, J. C.; Armentrout, P. B. *J. Phys. Chem. A* **2000**, *104*, 11420.

(7) More, M. B.; Ray, D.; Armentrout, P. B. *J. Am. Chem. Soc.* **1999**, *121*, 417.
(8) Fujii, T. *Mass Spectrom. Rev.* **2000**, *19*, 111.
(9) Hoyau, S.; Norrman, K.; McMahon, T. B.; Ohanessian, G. *J. Am. Chem. Soc.* **1999**, *121*, 8864.
(10) McMahon, T. B.; Ohanessian, G. *Chem.—Eur. J.* **2000**, *6*, 2931.
(11) Rodgers, M. T. *J. Phys. Chem. A* **2001**, *105*, 8145.
(12) Rodgers, M. T. *J. Phys. Chem. A* **2001**, *105*, 2374.
(13) Bojesen, G.; Breindahl, T.; Andersen, U. N. *Org. Mass Spectrom.* **2005**, *28*, 1448.
(14) Kish, M. M.; Ohanessian, G.; Wesdemiotis, C. *Int. J. Mass Spectrom.* **2003**, *227*, 509.
(15) Rodgers, M. T.; Armentrout, P. B. *Acc. Chem. Res.* **2004**, *37*, 989.
(16) Cooks, R. G.; Patrick, J. S.; Kotiaho, T.; McLuckey, S. A. *Mass Spectrom. Rev.* **1994**, *13*, 287.
(17) Cooks, R. G.; Wong, P. S. H. *Acc. Chem. Res.* **1998**, *31*, 379.
(18) Ervin, K. M.; Armentrout, P. B. *J. Chem. Phys.* **1985**, *83*, 166.
(19) Muntean, F.; Armentrout, P. B. *J. Chem. Phys.* **2001**, *115*, 1213.
(20) Moision, R. M.; Armentrout, P. B. *J. Am. Soc. Mass Spectrom.* **2007**, *18*, 1124.
(21) Kim, T.; Tolmachev, A. V.; Harkewicz, R.; Prior, D. C.; Anderson, G.; Udseth, H. R.; Smith, R. D. *Anal. Chem.* **2000**, *72*, 2247.
(22) Ye, S. J.; Armentrout, P. B. *J. Phys. Chem. A* **2008**, *112*, published online March 26, http://dx.doi.org/10.1021/jp710709j.
(23) Teloy, E.; Gerlich, D. *Chem. Phys.* **1974**, *4*, 417.
(24) Gerlich, D. *Adv. Chem. Phys.* **1992**, *82*, 1.
(25) Aristov, N.; Armentrout, P. B. *J. Phys. Chem.* **1986**, *90*, 5135.
(26) Dalleska, N. F.; Honma, K.; Sunderlin, L. S.; Armentrout, P. B. *J. Am. Chem. Soc.* **1994**, *116*, 3519.
(27) Beyer, T. S.; Swinehart, D. F. *Commun. ACM* **1973**, *16*, 379.
(28) Stein, S. E.; Rabinovitch, B. S. *J. Chem. Phys.* **1973**, *58*, 2438.
(29) Stein, S. E.; Rabinovitch, B. S. *Chem. Phys. Lett.* **1977**, *49*, 183.
(30) Gilbert, R. G.; Smith, S. C. *Theory of Unimolecular and Recombination Reactions*; Blackwell Scientific: London, 1990.
(31) Robinson, P. J.; Holbrook, K. A. *Unimolecular Reactions*; Wiley-Interscience: New York, 1972.
(32) Rodgers, M. T.; Ervin, K. M.; Armentrout, P. B. *J. Chem. Phys.* **1997**, *106*, 4499.
(33) Rodgers, M. T.; Armentrout, P. B. *J. Chem. Phys.* **1998**, *109*, 1787.
(34) Hales, D. A.; Lian, L.; Armentrout, P. B. *Int. J. Mass Spectrom. Ion Processes* **1990**, *102*, 269.
(35) More, M. B.; Ray, D.; Armentrout, P. B. *J. Phys. Chem. A* **1997**, *101*, 831.
(36) Armentrout, P. B.; Simons, J. *J. Am. Chem. Soc.* **1992**, *114*, 8627.
(37) Moision, R. M.; Armentrout, P. B. *J. Phys. Chem. A* **2002**, *106*, 10350.
(38) Pearlman, D. A.; Case, D. A.; Caldwell, J. W.; Ross, W. R.; Cheatham, T. E.; DeBolt, S.; Ferguson, D.; Seibel, G.; Kollman, P. *Comput. Phys. Commun.* **1995**, *91*, 1.
(39) Bylaska, E. J.; de Jong, W. A.; Kowalski, K.; Straatsma, T. P.; Valiev, M.; Wang, D.; Aprà, E.; Windus, T. L.; Hirata, S.; Hackler, M. T.; Zhao, Y.; Fan, P.-D.; Harrison, R. J.; Dupuis, M.; Smith, D. M. A.; Nieplocha, J.; Tipparaju, V.; Krishnan, M.; Auer, A. A.; Nooijen, M.; Brown, E.; Cisneros, G.; Fann, G. I.; Früchtl, H.; Garza, J.; Hirao, K.; Kendall, R.; Nichols, J. A.; Tsemekhman, K.; Wolinski, K.; Anchell, J.; Bernholdt, D.; Borowski, P.; Clark, T.; Clerc, D.; Dachsel, H.; Deegan, M.; Dyall, K.; Elwood, D.; Glendening, E.; Gutowski, M.; Hess, A.; Jaffe, J.; Johnson, B.; Ju, J.; Kobayashi, R.; Kutteh, R.; Lin, Z.; Littlefield, R.; Long, X.; Meng, B.; Nakajima, T.; Niu, S.; Pollack, L.; Rosing, M.; Sandrone, G.; Stave, M.; Taylor, H.; Thomas, G.; Lenthe, J. v.; Wong, A.; Zhang, Z. *Nwchem, A Computational Chemistry Package for Parallel Computers*, version 4.5 ed.; Pacific Northwest National Laboratory: Richland, Washington 99352, 2003.
(40) Frisch, M. J.; Trucks, G. W.; Schlegel, H. B.; Scuseria, G. E.; Robb, M. A.; Cheeseman, J. R.; Montgomery, J. A., Jr.; Vreven, T.; Kudin, K. N.; Burant, J. C.; Millam, J. M.; Iyengar, S. S.; Tomasi, J.; Barone, V.; Mennucci, B.; Cossi, M.; Scalmani, G.; Rega, N.; Petersson, G. A.; Nakatsuji, H.; Hada, M.; Ehara, M.; Toyota, K.; Fukuda, R.; Hasegawa, J.; Ishida, M.; Nakajima, T.; Honda, Y.; Kitao, O.; Nakai, H.; Klene, M.; Li, X.; Knox, J. E.; Hratchian, H. P.; Cross, J. B.; Bakken, V.; Adamo, C.; Jaramillo, J.; Gomperts, R.; Stratmann, R. E.; Yazyev, O.; Austin, A. J.; Cammi, R.; Pomelli, C.; Ochterski, J. W.; Ayala, P. Y.; Morokuma, K.; Voth, G. A.; Salvador, P.; Dannenberg, J. J.; Zakrzewski, V. G.; Dapprich, S.; Daniels, A. D.; Strain, M. C.; Farkas, O.; Malick, D. K.; Rabuck, A. D.; Raghavachari, K.; Foresman, J. B.; Ortiz, J. V.; Cui, Q.; Baboul, A. G.; Clifford, S.; Cioslowski, J.; Stefanov, B. B.; Liu, G.; Liashenko, A.; Piskorz, P.; Komaromi, I.; Martin, R. L.; Fox, D. J.; Keith, T.; Al-Laham, M. A.; Peng, C. Y.; Nanayakkara, A.; Challacombe, M.; Gill, P. M. W.; Johnson, B.; Chen, W.; Wong, M. W.; Gonzalez, C.; Pople, J. A. *Gaussian 03*, revision B.02; Gaussian, Inc.: Pittsburgh, PA, 2003.
(41) Montgomery, J. A., Jr.; Frisch, M. J.; Ochterski, J. W.; Petersson, G. A. *J. Chem. Phys.* **1999**, *110*, 2822.
(42) Boys, S. F.; Bernardi, R. *Mol. Phys.* **1970**, *19*, 553.
(43) van Duijneveldt, F. B.; van Duijneveldt de Rijdt, J. G. C. M.; van Lenthe, J. H. *Chem. Rev.* **1994**, *94*, 1873.
(44) Wong, C. H. S.; Siu, F. M.; Ma, N. L.; Tsang, C. W. *THEOCHEM* **2002**, *588*, 9.
(45) Feller, D.; Glendening, E. D.; Woon, M. W.; Feyereisen, J. *J. Chem. Phys.* **1995**, *103*, 3526.
(46) Feller, D. *Chem. Phys. Lett.* **2000**, *322*, 543.
(47) Clarke, S. *Ageing Res. Rev.* **2003**, *2*, 263.
(48) Robinson, N. E.; Robinson, A. B. *Proc. Natl. Acad. Sci. U.S.A.* **2001**, *98*, 944.
(49) Dayhoff, M. O. *Atlas of Protein Sequences and Structures*; National Biomedical Research Foundation: Silver Spring, MD, 1969.
(50) Heaton, A. L.; Ye, S. J.; Armentrout, P. B. *J. Phys. Chem. A* **2008**, *112*, 3328.
(51) Lifshitz, C. *Adv. Mass Spectrom.* **1989**, *11A*, 713.
(52) Amicangelo, J. C.; Armentrout, P. B. *J. Phys. Chem. A* **2004**, *108*, 10698.